

Quantifying Gyrotropy in Magnetic Reconnection

M. Swisdak*

IREAP, University of Maryland, College Park MD 20742-3511, USA

(Dated: September 10, 2022)

A new scalar measure of the gyrotropy of a pressure tensor is defined. Previously suggested measures are shown to provide non-physical results in some cases. As examples of its applicability, the new measure is calculated for electron data taken from numerical simulations of magnetic reconnection and shown to sharply outline the separatrices and X-points. Such a diagnostic is potentially useful for spacecraft observations and so a method for calculating it from measurements made in an arbitrary coordinate system is presented.

I. INTRODUCTION

As commonly understood, magnetic reconnection refers to a process whereby the energy of the embedded field is transferred to the surrounding plasma via bulk acceleration and Ohmic dissipation. While frequently associated with changes in the topology of the magnetic field, formulating a precise general definition of reconnection is a surprisingly subtle task [1].

In what are known as 2.5D geometries, where variations in one direction are suppressed, the reduced dimensionality, coupled with the divergence-free nature of the magnetic field, allows field lines to be completely characterized as contours of a scalar function, ψ . (ψ is equivalent to the component of the magnetic vector potential in the invariant direction.) In this case, saddle points of ψ , known as X-points, mark locations of both topological change and magnetic reconnection. For fully three-dimensional systems, field lines can no longer be described by a single function and the definition of reconnection becomes significantly more complex. Finding the locations where magnetic reconnection occurs is non-trivial, even in numerical simulations [2–4].

Yet simulations have the luxury of a synoptic view with, in principle, access to the complete description of the plasma at any point in the domain. Spacecraft observations, in contrast, must make due with a limited set of measurements available from, at most, a few locations. The topological identification of reconnection sites is non-local in nature and hence extremely difficult to implement with these restrictions. Determinations must instead be based on local measurements of the electromagnetic fields and particles.

Due to their small Larmor radii and brief gyroperiods, electrons are closely tied to the magnetic field, much more so than the heavier ions. By streaming for long distances along field lines electrons efficiently probe magnetic structure; locations of topological interest, such as reconnection sites, should leave signatures in electron measurements. In this paper we present a diagnostic that quantifies these signatures and demonstrate, through numerical simulations, that it faithfully maps the regions

associated with magnetic reconnection.

II. MEASURING GYROTROPY

Given a distribution function $f(\mathbf{x}, \mathbf{v})$ that describes the density of particles with mass m in a phase space defined by position (\mathbf{x}) and velocity (\mathbf{v}), the pressure \mathbb{P} can be defined as

$$\mathbb{P} = m \int \mathbf{w} \mathbf{w} f d^3 \mathbf{v}, \quad (1)$$

where $\mathbf{w} = \mathbf{v} - \bar{\mathbf{v}}$ is the velocity relative to the mean flow $\bar{\mathbf{v}}$. While \mathbb{P} is, in general, a tensor with six independent components, it can be characterized by a single scalar when f is spherically symmetric (e.g., a Maxwellian). A magnetic field, by imposing a preferred direction, can produce a cylindrically symmetric, or gyrotropic, distribution. In this case the pressure tensor takes the form

$$\mathbb{P} = P_{\parallel} \hat{\mathbf{b}} \hat{\mathbf{b}} + P_{\perp} (\mathbb{I} - \hat{\mathbf{b}} \hat{\mathbf{b}}), \quad (2)$$

where $\hat{\mathbf{b}} = |\mathbf{B}|/B$ is a unit vector in the direction of the magnetic field, P_{\parallel} and P_{\perp} are scalars, and \mathbb{I} is the unit tensor. In the equivalent matrix formulation,

$$\mathbb{P} = \begin{pmatrix} P_{\parallel} & 0 & 0 \\ 0 & P_{\perp} & 0 \\ 0 & 0 & P_{\perp} \end{pmatrix} \quad (3)$$

Observationally, pressure tensors are never completely gyrotropic because they include non-zero off-diagonal components, although these are often much smaller than the diagonal terms. Since departures from gyrotropy are expected to be associated with locations of magnetic reconnection, a quantitative measure of this smallness would be useful.

With this goal in mind, others have suggested possible diagnostics. Scudder and Daughton [5] proposed a measure, dubbed the agyrotropy and denoted $A\mathcal{O}_e$, that characterizes a distribution function's weighted average of dispersions of velocities perpendicular to the local field direction (see Appendix A of their paper for a full description). It varies between 0 and 2 with the minimum supposedly corresponding to gyrotropic distributions. However, as demonstrated below, there exist agyrotropic pressure tensors for which $A\mathcal{O}_e = 0$.

* swisdak@umd.edu

Aunai et al. [6] proposed another measure, denoted D_{ng} and named non-gyrotropy. It is proportional to the root-mean-square of the off-diagonal elements of the pressure tensor normalized by the local thermal energy. As with the agyrotropy, $D_{ng} = 0$ for a gyrotropic distribution but, as also shown below, there exist pressure tensors with maximal departures from gyrotropy for which D_{ng} is arbitrarily close to 0.

A brief mathematical digression is necessary in order to justify a better measure. The matrix representations of pressure tensors must satisfy certain constraints because they originate as moments of distribution functions. Specifically, a physically meaningful pressure tensor is a real 3×3 symmetric matrix (i.e., $P_{ij} = P_{ji}$) with positive eigenvalues. (Zero eigenvalues occur only in the zero-temperature limit. Since their inclusion complicates the discussion without adding enlightenment they will be ignored here.). This follows from the requirement that after diagonalization (which is always possible for a symmetric matrix) the non-zero matrix elements are both the eigenvalues of the tensor and the components of the pressure along the basis vectors of the rotated frame. For physical distributions the latter, and hence the former, must be positive. Matrices possessing these properties are called symmetric positive-definite. (Not to be confused with positive matrices, for which each matrix element is positive. The off-diagonal elements of a pressure tensor can be negative.)

Defining a scalar measure of gyrotropy requires a result from the theory of symmetric positive-definite matrices. Sylvester's criterion [7] states that for such matrices the determinants of all of the upper-left submatrices (i.e., the leading principal minors) must be positive. A pressure tensor with gyrotropic diagonal, but non-zero off-diagonal, entries can be written as

$$\mathbb{P} = \begin{pmatrix} P_{\parallel} & P_{12} & P_{13} \\ P_{12} & P_{\perp} & P_{23} \\ P_{13} & P_{23} & P_{\perp} \end{pmatrix} \quad (4)$$

In this representation one of the coordinate axes points in the direction of the local field and the others are oriented such that the final two components of the diagonal of \mathbb{P} are equal. For matrices of this form Sylvester's criterion implies the inequalities

$$P_{12}^2 \leq P_{\parallel} P_{\perp} \quad P_{13}^2 \leq P_{\parallel} P_{\perp} \quad P_{23}^2 \leq P_{\perp}^2 \quad (5)$$

The converse does not hold: satisfaction of these inequalities does not guarantee that \mathbb{P} is positive-definite or a valid pressure tensor.

A slight manipulation of the inequalities yields a natural definition for a measure of gyrotropy:

$$Q = \frac{P_{12}^2 + P_{13}^2 + P_{23}^2}{P_{\perp}^2 + 2P_{\perp}P_{\parallel}} \quad (6)$$

For gyrotropic tensors $Q = 0$, while for maximally departures from gyrotropy $Q = 1$. In general, the coordinate

system in which \mathbb{P} is measured does not align with the local magnetic field and so \mathbb{P} is usually not in the form given by equation 4. While it is always possible to rotate \mathbb{P} into a frame aligned with the local field, Appendix A demonstrates how to calculate Q without such a transformation by using tensor invariants.

Sylvester's criterion provides a firm mathematical basis for the definition of Q . With it in mind, it is possible to construct pressure tensors for which other previously proposed measures give physically unreasonable results. Consider a system with a pressure tensor, of the type shown in equation 4, given by

$$\mathbb{P} = \begin{pmatrix} 1 & 1/2 & 0 \\ 1/2 & 1 & 0 \\ 0 & 0 & 1 \end{pmatrix} \quad (7)$$

Since \mathbb{P} has eigenvalues of $1/2$, 1 , and $3/2$, it is positive-definite and hence physically valid. Yet, despite the off-diagonal elements that make it clearly not gyrotropic,

$$A\mathcal{O}_e = 0 \quad (8)$$

In fact $A\mathcal{O}_e = 0$ for any positive-definite \mathbb{P} in the form of equation 4 with $P_{23} = 0$, irrespective of the other off-diagonal components. For reference, $\sqrt{Q} = \sqrt{3}/6$ and $D_{ng} = \sqrt{2}/3$ in this case. (The other gyrotropy measures considered here scale as ratios of first powers of pressure components while Q scales quadratically. The subsequent discussion, where necessary to ensure a fair comparison, uses \sqrt{Q} .) A coordinate rotation about the magnetic field direction will redistribute the off-diagonal components, but will not change the values of the measures. The vanishing of $A\mathcal{O}_e$ suggests that it does not, in all cases, correctly describe a pressure tensor's gyrotropy.

The nongyrotropy measure proposed by Aunai et al. [6], D_{ng} , is defined as

$$D_{ng} = \frac{\sqrt{8(P_{12}^2 + P_{13}^2 + P_{23}^2)}}{P_{\parallel} + 2P_{\perp}} \quad (9)$$

The most significant difference between it and \sqrt{Q} occurs in the normalization, which for D_{ng} is to the thermal energy, $P_{\perp} + P_{\parallel}/2$. As with the other measures, $D_{ng} = 0$ for gyrotropic tensors. The maximum value of D_{ng} can be shown to be $\sqrt{8/3}$; rescaling to make it unity is trivial, but diminishes the physical motivation of the normalization

A more significant issue arises in consideration of the pressure tensor

$$\mathbb{P} = \begin{pmatrix} 1 & \sqrt{x} & \sqrt{x} \\ \sqrt{x} & x(1+\epsilon) & x \\ \sqrt{x} & x & x(1+\epsilon) \end{pmatrix} \quad (10)$$

where $0 < \epsilon \ll 1$ and $x > 0$. The eigenvalues of \mathbb{P} , all positive, are $\approx 1 + 2x$, $\approx \epsilon x/(1 + 2x)$, and ϵx . Some

algebra yields

$$D_{ng} = \frac{\sqrt{8(2x+x^2)}}{1+2x(1+\epsilon)} \quad (11)$$

$$Q = \frac{1}{1+\epsilon} \left(\frac{2+x}{2+x(1+\epsilon)} \right) \quad (12)$$

As $\epsilon \rightarrow 0$, the pressure tensor becomes maximally non-gyrotropic, but D_{ng} does not approach its maximal value. In particular, $D_{ng} \rightarrow 4\sqrt{x}$ and becomes arbitrarily small as $x \rightarrow 0$. In contrast, $Q \rightarrow 1$ as $\epsilon \rightarrow 0$ for arbitrary x . (For completeness, $A\varnothing_e = 2/(1+\epsilon)$ for this case and also approaches its maximal value as $\epsilon \rightarrow 0$.) This inappropriate limit of D_{ng} , a consequence of the normalization to the thermal energy, demonstrates that it also does not provide a complete measure of gyrotropy.

III. SIMULATIONS

To test Q 's usefulness as a proxy for the identification of reconnection sites, we turn to numerical simulations, specifically particle-in-cell simulations that can calculate the full pressure tensor. Here we use the code `p3d` [8]. It employs normalized units based on a field strength B_0 and density n_0 , with lengths normalized to the ion inertial length $d_i = c/\omega_{pi}$ where ω_{pi} is the ion plasma frequency, times to the ion cyclotron time Ω_{i0}^{-1} , and velocities to the Alfvén speed c_{A0} .

A. Run 1: Anti-Parallel Reconnection

As a first case, we consider a variation of the standard GEM Challenge [9]. The simulation domain has dimensions $(L_x, L_y) = (51.2, 25.6)$ with an initial magnetic field of $B_x = \tanh(y/w_0)$ and $w_0 = 0.5$. There is no field component in the z direction (i.e., this is anti-parallel reconnection). To ensure pressure balance, the density $n = n_b + \text{sech}^2(y/w_0)$, where $n_b = 0.2$, and the electron and ion temperatures are initially isotropic with $T_e = 1/12$ and $T_i = 5/12$. The ion-to-electron mass ratio is 400 (thus implying d_e/d_i , the ratio of electron and ion inertial lengths, is $1/20$) and the speed of light is 40. The spatial grid has resolution $\Delta x = 1/160$ and so there are 8 gridpoints per electron inertial length and ≈ 3 per electron Larmor radius in the maximum field. There are 100 particles per cell for each species in the asymptotic region and $\approx 4 \times 10^9$ in the entire domain.

Figure 1 shows a comparison between \sqrt{Q} and $A\varnothing_e$ during a time of steady reconnection (as discussed in Section IV, D_{ng} closely follows \sqrt{Q} and so is not plotted). Only a fraction of the simulation domain, centered on the X-point, is pictured in order to highlight the regions exhibiting strong departures from gyrotropy. On the right-hand side of each image are the traces of two cuts, one through the X-point (blue) and the other $\approx 5d_i = 100d_e$ downstream (red). Both $A\varnothing_e$ and Q are significant near

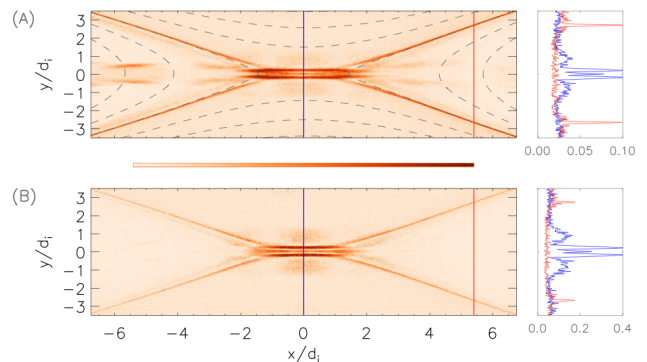


FIG. 1. Images of \sqrt{Q} (panel A) and $A\varnothing_e$ (panel B) with superimposed magnetic field lines (dotted) for the run described in section III A. Colors represent different values in each image; the central bar shows the relative variation. The data have been averaged over $0.03\Omega_{ci}^{-1} = 12\Omega_{ce}^{-1}$, or ≈ 2 electron Larmor orbits in the asymptotic field. The panels on the right show cuts along the corresponding colored lines in the main images.

the X-point, although there are minor differences in the aspect ratio and structural details of the bright regions. The bifurcation at $y/d_i = 0$ and $-2 \lesssim x/d_i \lesssim 2$ mirrors that seen in the charge and current densities (not shown) and reflects the complicated dynamics of Speiser particle orbits near the region of null field.

The magnitudes of \sqrt{Q} and $A\varnothing_e$ near the X-point (blue peaks in the right panels) are not directly comparable, in part because the two measures have different maximal values. The more meaningful comparison is between the sizes of the X-point peaks and the measure's respective asymptotic values. These are roughly equal. On the other hand, the magnetic separatrices (red peaks) are comparatively much weaker in $A\varnothing_e$ and stronger in \sqrt{Q} . Since the separatrices mark topological boundaries and should exhibit strong departures from gyrotropy the small values of $A\varnothing_e$ are likely related to the deficiency highlighted in the discussion following equation 7.

Both measures show small departures from gyrotropy in the humps in the blue curves just upstream of the X-point. These may arise from decreases in P_\perp (due to magnetic moment conservation) followed by scattering to other components. Another possibility is that beams of inflowing electrons, when superimposed on the base Maxwellian, drive the distribution function away from cylindrical symmetry.

B. Run 2: Guide Field Reconnection

As a second case we consider a force-free equilibrium where the initial density ($n = 1$) and temperatures ($T_i = T_e = 1/8$) have no spatial variations. The reconnecting field has the form $B_x = \tanh(y/w_0)$, here with $w_0 = 1$, but now the out-of-plane (guide) component B_z varies so that $B_x^2 + B_z^2$ is constant. The ini-

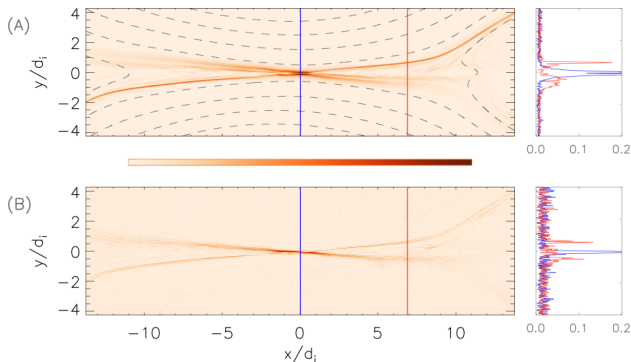


FIG. 2. Images of \sqrt{Q} (panel A) and $A\mathcal{O}_e$ (panel B), in the same format as Figure 1, for the run described in section III B. The data have been averaged over $0.5\Omega_{ci}^{-1} = 12.5\Omega_{ce}^{-1}$.

tial guide field is asymptotically 2 and rises to $\sqrt{5}$ at the current sheet's center. The domain has dimensions $(L_x, L_y) = (51.2, 25.6)$, the ion-to-electron mass ratio is 25 and the speed of light is 15. The spatial grid has resolution $\Delta x = 1/40$, which implies 8 gridpoints per electron inertial length and ≈ 2 per electron Larmor radius in the maximum field. There are 100 particles per cell for each species and $\approx 2 \times 10^9$ in the entire domain.

Figure 2, in the same format as Figure 1, shows the region near the X-point. Both \sqrt{Q} and $A\mathcal{O}_e$ peak there, although again the morphologies in the downstream region exhibits differences. The asymmetry between the separatrices, a common feature of guide field reconnection, is apparent in the images. As in Figure 1, the cuts show that the separatrices are somewhat stronger in \sqrt{Q} than in $A\mathcal{O}_e$. In images of the entire domain (not shown), the enhancement of \sqrt{Q} on the upper-right and lower-left separatrix continues around nearly the entire exterior of the downstream magnetic island while $A\mathcal{O}_e$ quickly peters out. However, perhaps the strongest difference is in the background noise level. While the two measures have similar peak-to-background ratios for the simulation of Section III A, here they differ by a factor of ≈ 4 , with \sqrt{Q} smoother than in Figure 1 and $A\mathcal{O}_e$ noisier. The improvement in \sqrt{Q} can be attributed to the strong guide field and its driving of the plasma towards gyrotropy. Finally, the indentation in the magnetic field lines at $x/d_i \approx 11$ is a transient feature due to the interaction of the outflowing plasma and the remains of a small magnetic island expelled from the X-point earlier in the simulation.

IV. DISCUSSION

We have proposed a new, mathematically rigorous measure of the gyrotropy of an arbitrary pressure tensor and presented numerical simulations of 2.5D reconnection demonstrating that gyrotropy violations peak near magnetic topological boundaries. Testing the efficacy of Q in three-dimensional simulations and with spacecraft

data are obvious next steps. It is unlikely that any single diagnostic can unambiguously identify reconnection sites in spacecraft data, but Q offers a complementary approach to methods based on other measurements. The calculation of Q requires the full electron pressure tensor (which is available on the recently launched Magnetospheric Multiscale Mission) and can be easily performed in any coordinate system using the algorithm presented in Appendix A.

While Q has some similarities with previously proposed measures, particularly the non-gyrotropy parameter D_{ng} of Aunai et al. [6], there are pressure tensors (e.g., equation 10) for which only Q gives physically meaningful results. However, in many instances the difference between the two is relatively minor. Their ratio can be written as

$$\frac{Q}{D_{ng}^2} = \frac{(y+2)^2}{8(1+2y)} \quad (13)$$

where $y = P_{\parallel}/P_{\perp}$. The right-hand side takes its minimal value for $y = 1$ and only varies by $\approx 30\%$ for $0 \leq y \leq 4$. Although the ratio can become arbitrarily large when $y \rightarrow \infty$, approaching that limit in a physical system will trigger other effects. Of particular note is the firehose mode, for which the instability criterion is $\beta_{\perp}(y-1) = \beta_{\perp}(P_{\parallel}/P_{\perp} - 1) > 2$. Under normal circumstances plasmas cannot significantly exceed this threshold, which thus implies $y < 1 + 2/\beta_{\perp}$. As a consequence, the differences between D_{ng} and \sqrt{Q} are starkest for $\beta_{\perp} \ll 1$.

The differences between Q and the agyrotropy $A\mathcal{O}_e$ are more significant. The larger class of pressure tensors that $A\mathcal{O}_e$ mistakenly identifies as gyrotropic likely contributes to its relative weakness in illuminating magnetic separatrices (e.g., in panel B of Figure 2). Even though $A\mathcal{O}_e$ successfully identifies X-points in the two simulations presented here, the uncertainty surrounding what it actually measures raises questions about its use.

Finally, an interesting connection exists between \mathbb{P} and the inertia tensor of a rigid body. Since both are symmetric and positive-definite, a measure analogous to Q also exists for the former. To be relevant, however, something external to the body must define a preferred direction in a manner similar to the role the magnetic field plays in defining gyrotropy.

ACKNOWLEDGMENTS

We would like to acknowledge helpful conversations with K. Schoeffler. This work was supported by NASA grant NNX14AF42G.

Appendix A: Calculating Q

Beginning with a pressure tensor in an arbitrary coordinate system, the calculation of Q from equation 6

requires a transformation into a frame in which the diagonal components are in gyrotropic form. A tensor \mathbb{A} transforms under coordinate rotations according to the prescription

$$\mathbb{A}' = \mathbb{R}^T \mathbb{A} \mathbb{R} \quad (\text{A1})$$

where \mathbb{R} is a rotation matrix. (Both the symmetry of \mathbb{A} and its eigenvalues are preserved under rotation of the coordinate axes.) Properly chosen \mathbb{R} 's will transform an arbitrary pressure tensor into gyrotropic form, although the calculation is somewhat tedious.

An easier method relies on the fact that certain combinations of tensor elements are invariant under coordinate rotations. In particular, for a 3×3 tensor with elements P_{ij} there are three invariants. Of importance here are the trace

$$I_1 = P_{xx} + P_{yy} + P_{zz} \quad (\text{A2})$$

and the sum of principal minors

$$I_2 = P_{xx}P_{yy} + P_{xx}P_{zz} + P_{yy}P_{zz} - (P_{xy}P_{yx} + P_{xz}P_{zx} + P_{yz}P_{zy}) \quad (\text{A3})$$

Note that $P_{ij} = P_{ji}$ for symmetric matrices and so the final three terms of I_2 simplify. The third invariant, not used here, is the determinant.

With these definitions Q can be expressed in terms of I_1 , I_2 , and the parallel pressure P_{\parallel} , the latter of which can be easily calculated from the relation

$$\begin{aligned} P_{\parallel} &= \hat{\mathbf{b}} \cdot \mathbb{P} \cdot \hat{\mathbf{b}} \\ &= b_x^2 P_{xx} + b_y^2 P_{yy} + b_z^2 P_{zz} + \\ &\quad 2(b_x b_y P_{xy} + b_x b_z P_{xz} + b_y b_z P_{yz}) \end{aligned} \quad (\text{A4})$$

where b_i is the i^{th} component of the unit vector aligned with the local magnetic field. After some algebraic manipulations,

$$Q = 1 - \frac{4I_2}{(I_1 - P_{\parallel})(I_1 + 3P_{\parallel})} \quad (\text{A5})$$

In this form Q can be simply computed in an arbitrarily oriented coordinate system, without need for coordinate transformations and the associated matrix multiplications.

-
- [1] K. Schindler, M. Hesse, and J. Birn, *J. Geophys. Res.* **93**, 5547 (1988).
 - [2] J. C. Dorelli and A. Bhattacharjee, *Phys. Plasmas* **15**, 056504 (2008).
 - [3] A. L. Haynes and C. E. Parnell, *Phys. Plasmas* **17**, 092903 (2010).
 - [4] C. M. Komar, P. A. Cassak, J. C. Dorelli, A. Glocer, and M. M. Kuznetsova, *J. Geophys. Res.* **118**, 4998 (2013).
 - [5] J. Scudder and W. Daughton, *J. Geophys. Res.* **113**, A06222 (2008).
 - [6] N. Aunai, M. Hesse, and M. Kuznetsova, *Phys. Plasmas* **20**, 092903 (2013).
 - [7] G. Dahlquist and Å. Björck, *Numerical Methods* (Dover Publications, 2003), chap. 5, pp. 162–164.
 - [8] A. Zeiler, D. Biskamp, J. F. Drake, B. N. Rogers, M. A. Shay, and M. Scholer, *J. Geophys. Res.* **107**, 1230 (2002).
 - [9] J. Birn, J. F. Drake, M. A. Shay, B. N. Rogers, R. E. Denton, M. Hesse, M. Kuznetsova, Z. W. Ma, A. Bhattacharjee, A. Otto, et al., *J. Geophys. Res.* **106**, 3715 (2001).